3D Photonic Integrated Interposer Enabling Connectivity between Multi-Core Fibers and Photonic Integrated Circuits

Madeleine Weigel*[a], Martin Kresse[a], Crispin Zawadzki[a], Philipp Winklhofer[a], Lea Flach[a], Klara Mihov[a], Jakob Reck[a], David de Felipe[a], Tianwen Qian[a], Moritz Kleinert[a], Norbert Keil[a] and Martin Schell[a]

[a] Fraunhofer Institute for Telecommunication, Heinrich-Hertz-Institut, Einsteinufer 37, 10587 Berlin, Germany

ABSTRACT

The increasing bandwidth demands in data centers require optical transceivers that can provide aggregated capacities of 1.6 Tb/s and beyond. In spatial-division-multiplexing (SDM) for optical transceivers, multi-core fibers (MCF) enable the transport of different spatially separated channels on a shallow footprint. MCF cores are usually arranged in multiple layers, which poses a challenge for interfacing with conventional photonic integrated circuits (PICs) with only one waveguide propagation layer.

To address this challenge, a novel 3D photonic integrated interposer structure is proposed in this work for coupling the different layers of MCF cores with arrays of conventional 2D electro-absorption modulated lasers (EML) and photodetectors (PD). The interposer, developed on Fraunhofer HHI's polymer-based hybrid integration platform, contains 1x1 3D multimode interference (MMI) couplers. These novel 3D MMIs can interconnect a vertical pitch of 22.5 µm to match the large vertical distance of the MCF cores. MMI losses of 3 dB (best case) were measured for the fabricated MMIs at a wavelength of 1310 nm. This enables the connection of five MCFs with 8 cores each in an array to two arrays of 4 EMLs and two arrays of 4 PDs. We will discuss the design, and characterization of this 3D photonic integrated interposer in more detail.

Keywords: 3D photonic integration, Multi-mode interference coupler, Multi-core fiber, Interposer, Polymer-based waveguides

1. INTRODUCTION

The MCF plays an important role in meeting the data center's growing bandwidth requirements [1, 2]. Due to the optical SDM, optical transceivers with a capacity of 1.6 Tb/s, and beyond can be realized [3]. The multi-core fiber has several spatially separated single-mode fiber cores in its cross section, usually arranged in rows (Figure **1** a). Due to this arrangement, direct coupling with in-plane devices such as electro-absorptive modulator laser diode (EML) arrays and photodiode (PD) arrays is not possible. A 3D passive interposer device is required to bridge the vertical gap. Several systems for connecting 2D components to MCFs have been realized so far. A well-known type of device consists of waveguides written into a glass block using laser inscription [4]. In this process, the waveguide structures within the glass block are free forms, which are produced on a chip scale. The future of interfacing MCFs to in-plane devices requires 3D interposer structures fabricated on wafer scale due to the potential of high-volume and cost-efficient manufacturing. The 3D PolyBoard platform can fulfill this requirement by using 1x1 3D MMIs [5] as the basic building block. In addition, the design of the multi-layer waveguide routing network adapted to the components to be connected is possible. In the first step, the basic building block, the 1x1 3D MMI, which was already developed for smaller vertical distances , has to be adapted to the given requirements of the MCF coupling. The functionality of the vertical coupling between vertical stacked waveguide layers of the 1x1 3D MMI remains the same for the different requirements. Nevertheless, an adaption of the procedure of the development and the consideration of new parameters is essential for the 1x1 3D MMIs with the high vertical distance. The MMI height must now be modified to an external system, such as the vertical distances of the MCF cores. Figure 1 a) shows the cross section of a MCF with 4x2 cores. To enable an even distribution of losses between the cores, the routing is designed in such a way that a third waveguide layer (middle) is introduced (Figure 1 b) and thus the

* madeleine.weigel@hhi.fraunhofer.de; phone +493031002-283; hhi.fraunhofer.de

Integrated Optics: Devices, Materials, and Technologies XXIX, edited by Sonia M. García-Blanco, Pavel Cheben, Proc. of SPIE Vol. 13369, 1336919 · © 2025 SPIE
0277-786X · doi: 10.1117/12.3043661

vertical routing only has to take place over half of the vertical spacing of the cores of 22.5 µm. Figure 1 c) shows the entire interposer design for connecting an MCF array consisting of five fibers with 4x2 cores each to couple two 4-fold EML arrays as transmitting units and two 4-fold PD arrays as receiving units for an optical transceiver.

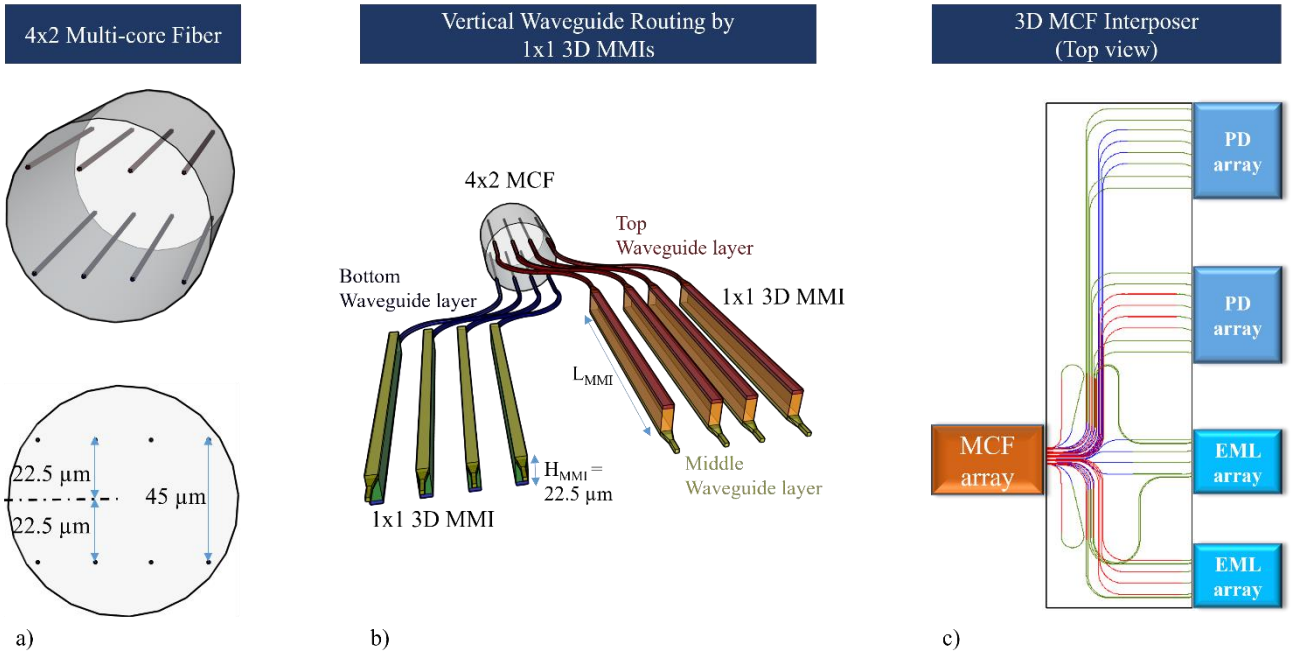

Figure 1. Overview of the development stages from the bare MCF and its cross-section (a) to the interposer design (c) for coupling in-plane PICs with an MCF array for the fabrication of an optical transceiver. The 3D visualization in the middle shows the vertical routing between the different waveguide layers using 1x1 3D MMIs (b) with a high vertical distance of 22.5 µm (center-to-center) between the layers. The 1x1 3D MMIs are the basic building blocks for realizing the 3D MCF interposer functionality. Each color change in a waveguide represents a change between layers.

The following sections initially focus on the development of the basic building block, the 1x1 3D MMI with a high vertical spacing. The simulation and the final design to realize a low-loss vertical coupling and a manufacturable design are examined in detail. The successfully manufactured 3D MCF interposer with 28 1x1 3D MMI is then evaluated in the characterization and a possible outlook for further development is given.

2. SIMULATION AND DESIGN

For the functionality of the MCF interposer, the basic building block, the 1x1 3D MMI with the high vertical spacing of 22.5 µm (center-to-center) is the main focus of this chapter. The following section briefly describes the functionality of the 1x1 3D MMIs. A single-mode waveguide guides the light with a target wavelength of 1310 nm to the vertical MMI region. Due to the refractive index contrast between the core and cladding of $\Delta n = 0.03$, the waveguide has a cross-section of 2.7 µm by 2.7 µm. The light is coupled into the MMI region. Due to the expansion of the core in the vertical direction, a multi-mode field is created by self-interference [6]. This field propagates vertically through the MMI region (Figure **4** a). By choosing suitable MMI parameters: height, length, and width, according to the self-imaging theory [6], spots can be found that are equal in intensity to the input intensity. The light is coupled out using a single-mode waveguide in the higher waveguide layer. The MMI length and width parameters must be determined for the new fixed MMI height a total of 25.2 µm using simulations. This procedure is the same as for the 1x1 3D MMIs with the smaller vertical distance [5].

First, the fixed variables are defined. The target wavelength for this application of the optical transceiver is set to 1310 nm by the EML and PD components. The refractive index contrast in the PolyBoard is $\Delta n = 0.03$. As a result of the dimensions of the waveguides and the target height of 22.5 µm, the vertical distance between the waveguide layers, which corresponds to the layer thickness of the MMI layer, must be 19.8 µm. In the following step, the MMI length is tuned for different MMI widths and the combination of the two parameters with the lowest losses is determined. For an ideal 1x1 3D MMI (Figure **2** b) with the high vertical distance for the parameter MMI length = 3222.8 µm and MMI width = 7.7 µm, the MMI losses

are the lowest with approx. 0.5 dB. The term “ideal” in the context of 1x1 3D MMIs describes that the cross-section of the waveguides and MMI layers is rectangular and the offset between the layers is 0 µm. Figure **2** a) shows the cross-section of the ideal 1x1 3D MMI in the area of the MMI section and the detailed length scan for the MMI width of 7.7 µm is shown in Figure **2** b) (blue line).

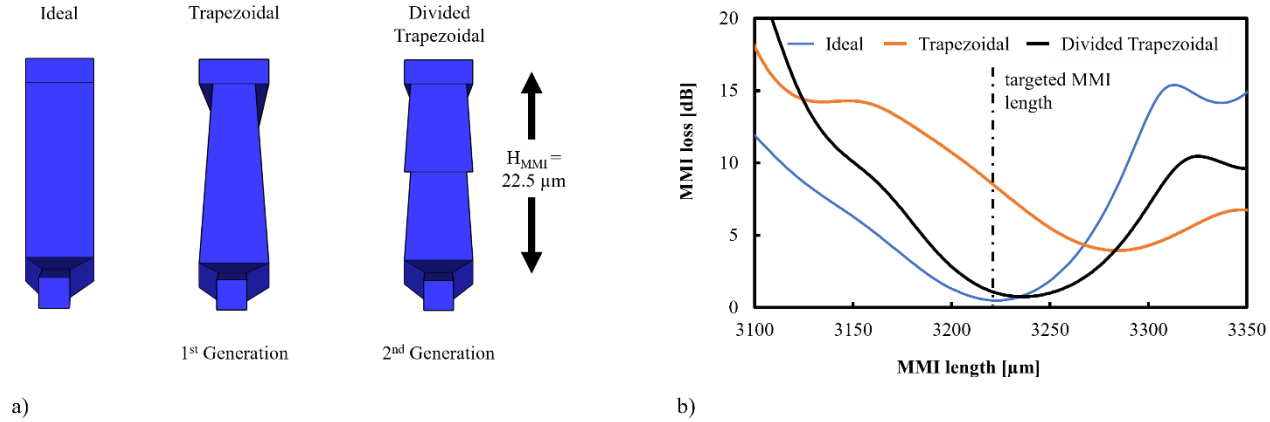

Figure 2. Overview of the 1x1 3D MMI cross sections of the MMI region (a), which were used to simulate the MMI losses as a function of the MMI length (b) for the fixed MMI height = 22.5 µm, MMI width = 7.7 µm and at the wavelength of 1310 nm.

Considering the 1x1 3D MMIs with smaller vertical spacing [5], the simulation at this point is not yet complete. In the next step, the technology parameters are defined and their influence on performance is further examined. Additional variables are introduced and investigated as technology parameters, which influence the structure of the 1x1 3D MMIs due to the selected fabrication process. These analyses extend the design target of low MMI losses to create a manufacturable design. In the first step, the technology parameter “offset” is considered [5]. An offset between the layer structures of the layers can occur in the 1x1 3D MMI with high vertical spacing. The offset is shown in the cross-section schematic in Figure **3**. The origin of this technology parameter is based on the layer structure in the fabrication of the MMI region. Figure **1** b) and Figure **2** a) show that the 1x1 3D MMIs consist of three layers: the lower waveguide layer, the MMI layer, and the upper waveguide layer.

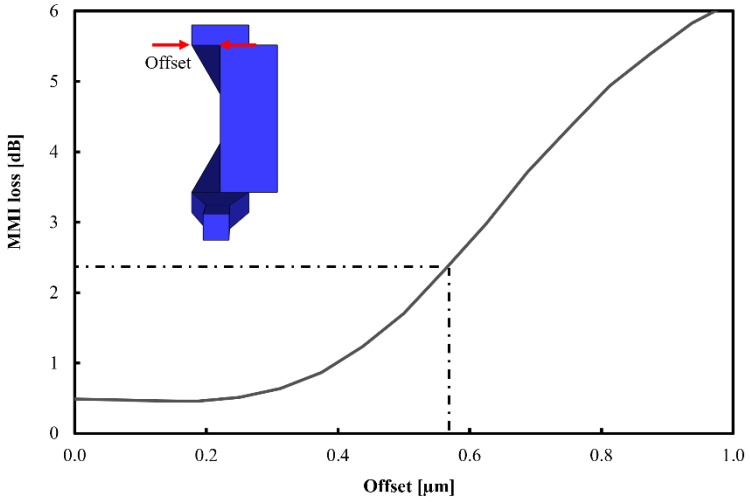

Figure 3. Simulation of the influence of the technology parameter offset (top left) for an ideal 1x1 3D MMI on the MMI losses.

In the UV lithography alignment process, these layers are aligned with each other using alignment marks. The accuracy of this alignment is approx. 1 µm [5, 7]. This peak value can often occur when aligning the MMI layer to the lower waveguide layer, as the vertical distance is greatest here and the shallow depth of field of the microscopes makes alignment more difficult. Therefore, the offset between these layers is usually considered. This technology parameter was examined for the given MMI width and length. In Figure **3**, can be seen that the offset has a significant influence on the performance of the 1x1 3D MMIs due to the high MMI length. The requirement is thus to keep the offset in the fabrication despite the significantly higher distance between the core layers < 1 µm. This requires a more precise implementation, especially in the control of the alignment during the lithography process. It will be shown in the visual inspection of the cross-section that this higher accuracy was achieved.

Due to the high vertical distance, however, the list of technology parameters for this type of 1x1 3D MMIs must be extended to include consideration of the influence of the cross-sectional shape of the MMI layer. The MMI layer has a target layer thickness of 19.8 µm. When structuring the core layer towards the MMI layer through etching using inductively coupled Plasma (ICP) in reactive-ion etching (RIE) mode with oxygen plasma, not only the MMI layer is etched in the vertical direction due to the long etching time, but also the already exposed side walls. As a result, the cross-sectional shape of the MMI layer deviates from the ideal rectangular to a trapezoidal shape (Figure **2** a). By reducing the etching time when adjusting the system parameters, the gradient of the trapezoidal shape can be reduced, but at the expense of the wall roughness, which leads to additional losses [7]. Based on this knowledge of the cross-sectional shape of the MMI layer, the simulation was adapted to investigate the influence of the shape on the performance of the 1x1 3D MMIs in more detail. The data on the slope of the trapezoid (Figure **2** a) were obtained from test etchings. Figure **2** b) shows the two extremes for the cross-sectional shape. In addition to the increase in MMI losses from 0.5 dB (ideal) to 4.3 dB (trapezoidal), a shift in the MMI length towards higher values can also be seen. The cause of the increase in MMI losses due to the MMI shape can be recognized by comparing the distribution of the spots with constructive interference within the entire MMI region and its propagation. The distribution of the spots with high intensity within the ideal 1x1 3D MMIs (Figure **4** a) shows a higher degree of symmetry than the trapezoidal shape (Figure **4** b).

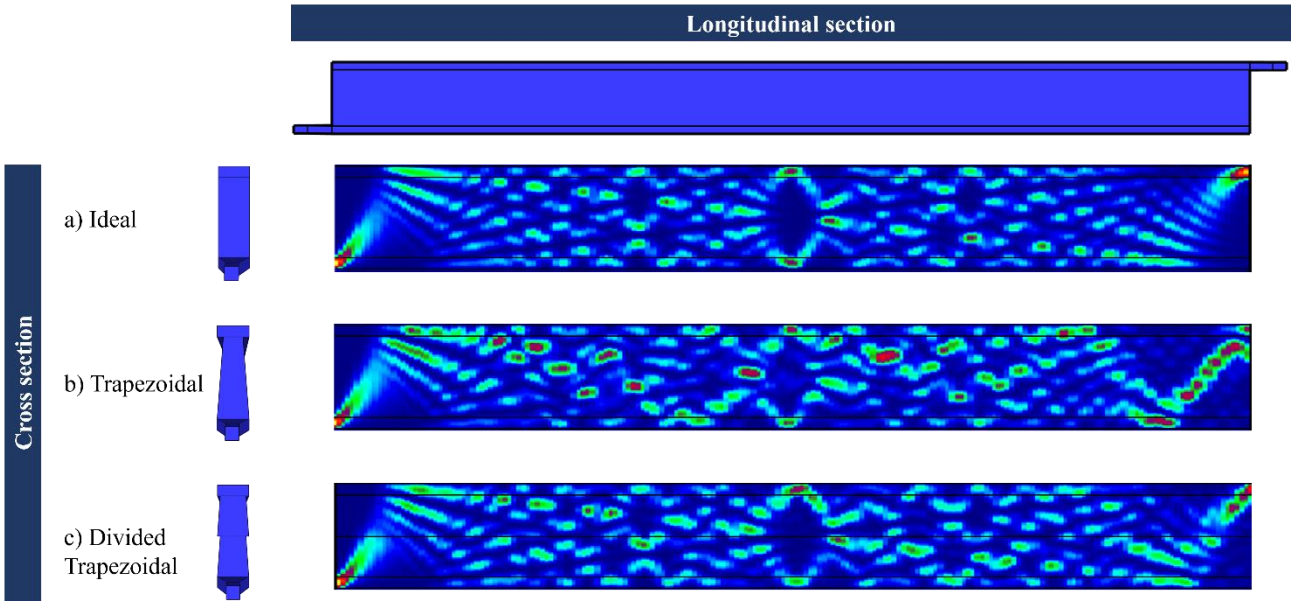

Figure 4. Simulation result of the propagation of the light field within the three layers (bottom waveguide, MMI, and top waveguide layer) in the MMI region of an 1x1 3D MMI for the three different MMI cross sections considered.

Due to the shape itself and the small overlap between the upper waveguide layer and the MMI layer, the system is disturbed, forming a lower degree of symmetry in the distribution. Furthermore, the coupling of the light from the upper waveguide to the MMI layer is reduced, and therefore, for short distances, modes are only guided in the upper waveguide. This changes the positions of constructive interference. In addition, at the end of the MMI layer (Figure **4** b), at the point where coupling into the single-mode output waveguide should occur, propagation is interrupted at the MMI and upper waveguide interface,

and reflection occurs in this area. The majority of the intensity therefore remains within the MMI layer. Fabrication of the MMI layer in just one process step is unsuitable for 1x1 3D MMIs with a high vertical distance.

A slight change in the procedure for fabrication of the MMI layer makes a significant difference to the situation described with the trapezoidal MMI layer. This change involves dividing the MMI layer vertically into two process steps and thus turning the trapezoidal shape into a divided trapezoidal shape. The influence of this procedure can be seen in Figure **2** b). With the same MMI length as for the ideal shape, the MMI losses are now approx. 1 dB. By increasing the overlap between the MMI layer and the upper waveguide layer (Figure **4** a), the distribution of the spots with constructive interference (Figure **4** c) is now much closer to that of the ideal 1x1 3D MMI. As a result, fabrication with a divided MMI layer in two process steps is preferable. An even smaller subdivision would not outweigh the significantly increased effort compared to the benefits and is therefore not recommended.

With this detailed consideration of the technology parameters, the 3D MCF interposer device with the 16 signal paths and an additional 16 alignment paths for coupling the components could be successfully fabricated.

3. CHARACTERIZATION

The polymer-based 3D MCF interposer was successfully realized as designed (Figure **1** c). The fabrication sequence for the 1x1 3D MMIs with high vertical distance differs from the previously developed process sequence [5, 7, 8] only in the subdivided MMI region. Figure **5** (left) shows a photograph of the fabricated interposer device. The characterization of this 3D PolyBoard was carried out in two stages. The first step is the visual inspection of the 3D MCF interposer. The top view is not informative enough for the contained 1x1 3D MMIs. Therefore, cross sectional images (Figure **5**) were created. The cross sections of the MMI regions can be seen in detail in Figure **5** (top right). Compared to the cross section from the simulation, the divided trapezoidal shape can be clearly seen, and thus the subdivision into the four layers. The fabricated MMI region is slightly higher than required, but still within the limits considering the manufacturing accuracy of the layer thicknesses of up to ± 0.6 µm for all four layers and the measurement accuracy of the method (± 0.3 µm). Furthermore, the cross section in Figure **5** shows that only a small offset of 0.6 µm has occurred. Within the scope of this visual inspection, the cross section shows a promising image for the functionality of the 1x1 3D MMIs within the MCF interposer.

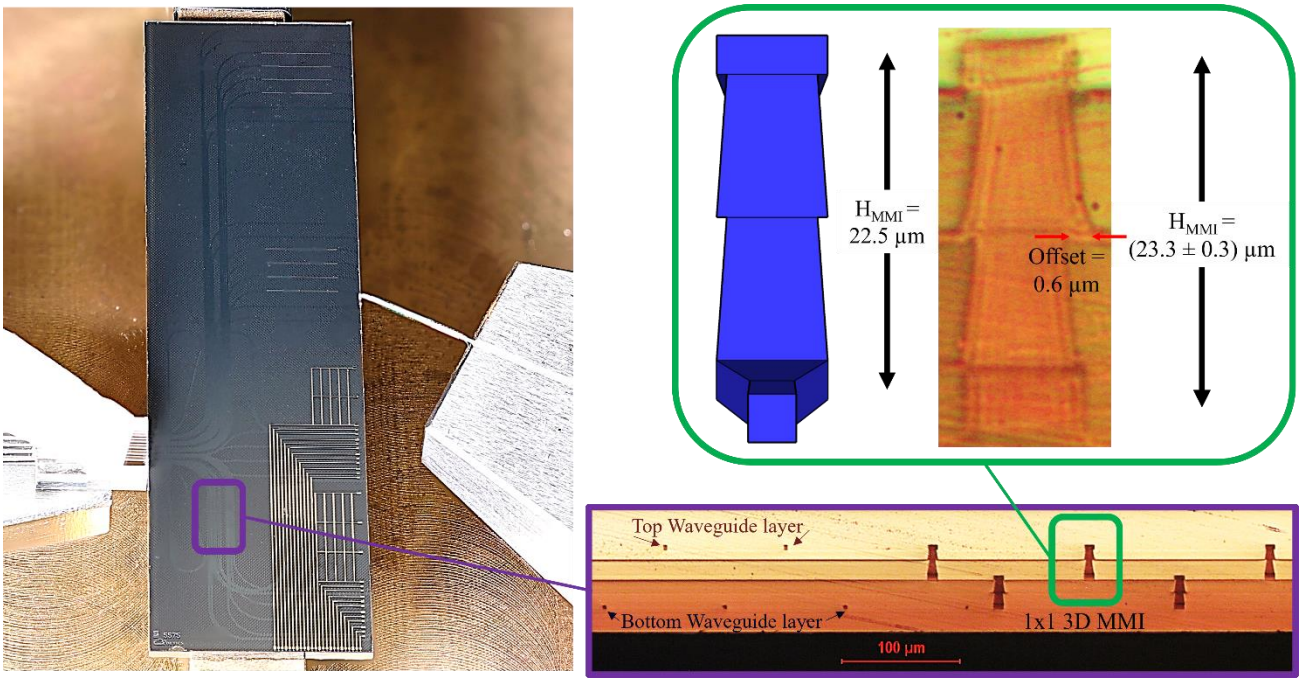

Figure 5. Fabricated 3D MCF interposer in top view with partially coupled MCF array with five fibers and the corresponding cross section of the waveguides in the different layers and MMI regions of 1x1 3D MMIs. The detailed view (top right) shows the measured data of a single 3D MMI region.

The second step of the characterization involves optical transmission measurements, which were carried out using the interposer. In order to examine the interposer and its waveguides as individual elements, lensed single-mode fibers were used to couple the light in and out. The measurement was carried out on the 28 interposer waveguide. Figure **6** a) shows the waveguide with the lowest insertion loss (including propagation and coupling losses) as a function of wavelength. After substracting the propagation and coupling losses, an MMI loss of approx. 2.4 dB at a wavelength of 1320 nm is obtained (Figure **6** a). The deviation of the losses of the 1x1 3D MMI from the simulation results is due to the offset between the waveguide and MMI layers. Figure **3** shows that the simulation results for the MMI loss of 2.4 dB (dashed line) indicate an offset of 0.6 µm. The comparison from the visual inspection of the MMI cross sections (Figure **5**) yielded the same offset. This shows that the results from these characterizations are consistent. Furthermore, it shows the agreement between the simulation and the results obtained from the manufactured device. The slight deviation of the wavelength with the minimum loss from the target wavelength of 1310 nm results from the height of the MMI region. Based on the self-imaging theory [6] and previous studies of 1x1 3D MMI with smaller vertical spacing [9], the slight increase compared to the target value (Figure **5**) causes the wavelength to be shifted to higher values.

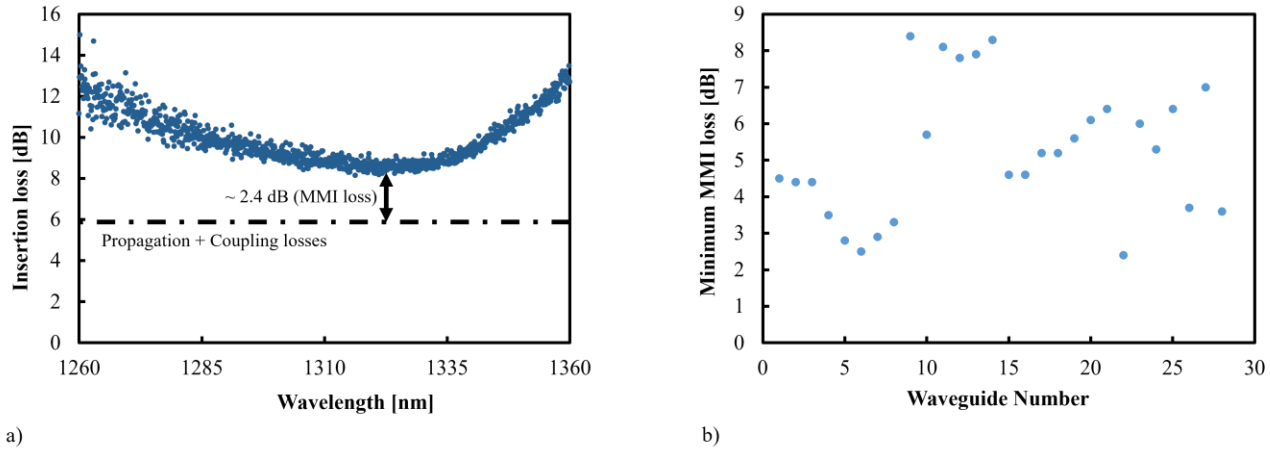

Figure 6. Transmission measurement of a single 3D MCF interposer waveguide (a) with 1x1 3D MMI lensed single-mode fiber to determine the MMI losses. The insertion losses given include propagation and coupling losses. For all waveguides of the interposer, the minimum MMI losses independent of wavelength are given in the diagram on the right (b). The MMI losses are shown excluding propagation and coupling losses.

The minimum MMI losses for each waveguide of the 3D MCF interposer are shown in Figure **6** b) graphically regardless of the wavelength. On average, the minimum MMI loss at 5.2 µm corresponds to an offset of approx. 0.8 µm (Figure **3**). This means that for most 1x1 3D MMIs of the interposer, the target of reducing the offset < 1 µm was met. The reason for the deviation between the 1x1 3D MMIs results lies, on the one hand, in the length of the interposer device at 33.5 mm and, on the other hand, in the topographies during the fabrication of the interposer. The device is fabricated on a 4-inch wafer. To produce a single polymer layer, the liquid polymer material is distributed on the wafer using spin-coating and then cured by UV light. The core layers are then structured. Due to the high thickness of the core layers, this process results in very high topography shapes and fluctuations in layer thickness. For the cladding layer, a planarization process in the fabrication sequence already exists. However, the planarization process is unsuitable for the core layers because of the increase in surface roughness [7] and the resulting additional losses [10]. This leads to partially different offsets between the 1x1 3D MMIs within a 3D MCF interposer, as well as a stronger deviation in MMI height and thus a resulting larger shift in wavelength with minimal MMI loss outside the considered spectrum. To improve this point, a planarization process with subsequent polishing needs to be developed so the core layers can also be planarized.

In the final step, the coupling with the MCF array was tested. The array in the coupling with the 3D MCF interposer is shown in Figure **5** (left). For the first tests, individual cores were coupled to the waveguides of the interposer (Figure **7** b). The differences in coupling losses between lensed single-mode fiber and the core of a MCF are negligible and overlap within the measurement accuracy (Figure **7**). Furthermore, a single 4x2 MCF could be successfully coupled with 8 interposer waveguides; the additional coupling loss for all eight cores of a MCF is 3 dB on average. Depending on the configuration of the MCF from the array and the selected coupling interface on the interposer, the losses can increase to

up to 10 dB. The variations between the different configurations can be attributed to the deviations of the MMI heights and the topographies on the wafer. So the coupling of several 4x2 MCFs from the array itself poses a challenge. Coupling up to 2 MCFs with the interposer was possible, but the coupling losses increased significantly. This illustrates that the match between the facet of the cores in the MCF array and the facet of the interposer decreases as the number of fibers increases, due to the points already mentioned.

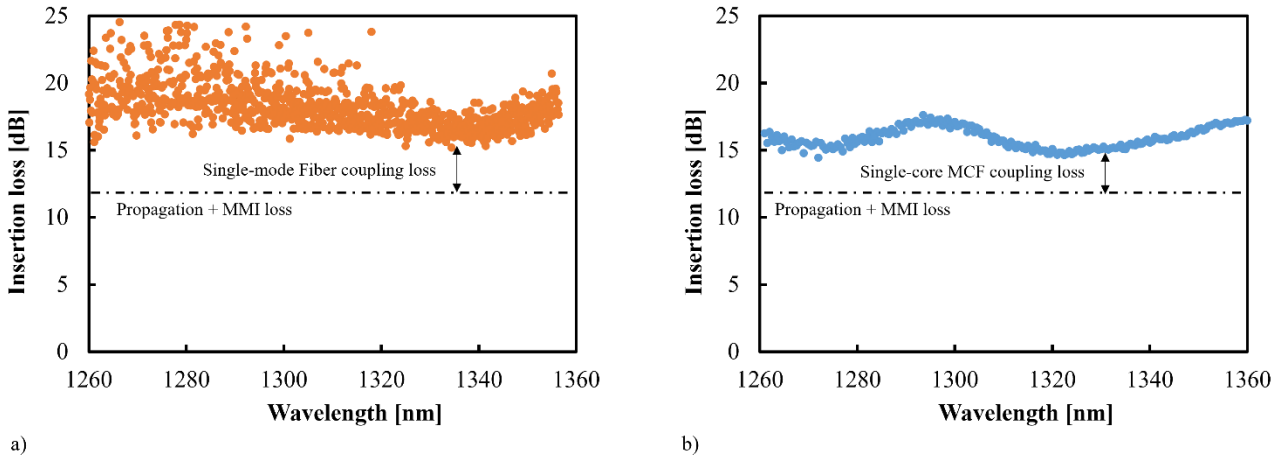

Figure 7. Comparison transmission measurement on the same 3D MCF interposer waveguide, once with lensed single-mode fiber (a) and once with a core of an MCF (b). The insertion losses given include propagation, MMI and coupling losses.

The successful fabrication of the 3D MCF interposer demonstrated here has already enabled the demonstration of the functionality of the optical transceiver with EML and PD arrays on a precursor module [2].

4. CONCLUSION

A 3D MCF interposer with 28 functional polymer-based waveguides with 1x1 3D MMIs with a high vertical distance of 22.5 µm (center-to-center) was successfully developed. The basic building blocks show a minimum MMI loss of 2.4 dB (best case) at a wavelength of 1320 nm and are the first of their kind. The comparison of simulation and measurement results showed a high level of consistency for this case, so there is good predictability for this 1x1 3D MMI. Coupling with individual 4x2 MCFs with the interposer device was also carried out successfully and showed an additional coupling loss of 3 dB. A further development of the fabrication process of the interposer to achieve a uniform coupling of the five fibers of the MCF array and to reduce the distribution of the MMI losses of the 1x1 3D MMIs, towards planarization of the core layer is necessary.

ACKNOWLEDGEMENTS

This work was partially funded by the European Commission through the project POETICS [contract number 871769] and through the project Sprinter [contract number 101070581].

REFERENCES

[1] E. Andrianopoulos *et al.*, "Hybrid Integration of Polymer PICs and InP Optoelectronics for WDM and SDM Terabit Intra-DC Optical Interconnects," in *2023 SBMO/IEEE MTT-S International Microwave and Optoelectronics Conference (IMOC)*, Castelldefels, Spain, 2023, pp. 259–261, doi: 10.1109/IMOC57131.2023.10379696.

[2] E. Andrianopoulos *et al.*, "Integrated 800 Gb/s O-band WDM optical transceiver enabled by hybrid InP-polymer photonic integration," *J. Opt. Commun. Netw.*, vol. 16, no. 8, D44, 2024, doi: 10.1364/JOCN.522903.
[3] T. Mizuno, H. Takara, A. Sano, and Y. Miyamoto, "Dense Space-Division Multiplexed Transmission Systems Using Multi-Core and Multi-Mode Fiber," *J. Lightwave Technol., JLT*, vol. 34, no. 2, pp. 582–592, 2016, doi: 10.1109/JLT.2015.2482901.
[4] R. R. Thomson *et al.*, "Ultrafast-laser inscription of a three dimensional fan-out device for multicore fiber coupling applications," *Optics express*, vol. 15, no. 18, pp. 11691–11697, 2007, doi: 10.1364/OE.15.011691.
[5] M. Nuck *et al.*, "Low-Loss Vertical MMI Coupler for 3D Photonic Integration," in *2018 European Conference on Optical Communication (ECOC)*, 2018, doi: 10.1109/ecoc.2018.8535479.
[6] L. B. Soldano and E. Pennings, "Optical multi-mode interference devices based on self-imaging: principles and applications," *J. Lightwave Technol., JLT*, vol. 13, no. 4, pp. 615–627, 1995, doi: 10.1109/50.372474.
[7] M. Weigel *et al.*, "Design and Fabrication of Crossing-free Waveguide Routing Networks using a Multi-layer Polymer-based Photonic Integration Platform," *J. Lightwave Technol., JLT*, pp. 1–7, 2023, doi: 10.1109/JLT.2023.3320908.
[8] Madeleine Nuck *et al.*, "3D photonic integrated 4x4 multi-mode interference coupler," in 2019, pp. 163–171, doi: 10.1117/12.2509776.
[9] M. Weigel, M. Kleinert, H. Conradi, A. Scheu, M. Kresse, C. Zawadzki, D. de Felipe, N. Keil, M. Schell, "3D Photonic Integration: Cascaded 1x1 3D Multi-mode Interference Couplers for Vertical Multi-layer Connections," *ECIO*. [Online]. Available: https://www.ecio-conference.org/wp-content/uploads/2020/06/11-madeleine-weigel-3d-photonic-integration-cascaded-1x1-3d-multi-mode-interference-couplers-ecio-2020.pdf
[10] G. T. Reed and A. P. Knights, *Silicon photonics: An introduction*. Chichester: John Wiley, 2010.